EFFECT OF CYLINDER SIZE ON HEAT TRANSFER BEHIND CIRCULAR CYLINDERS

Hajime FUSE and Shuichi TORII

(Received May 31, 1991)

Abstract

An experimental study was made on heat transfer and flow characteristics behind circular cylinders with three different sizes, 10mm, 12mm and 14mm in diameter, under lower freestream turbulence. The Nusselt number obtained, when the Reynolds number was kept a constant value, increased as the cylinder diameter became larger. Moreover, experimental results showed that for the relatively large cylinder case (D = 12mm), the laminar–to–turbulent transition region in the separated shear layer was shifted in the upstreamwise direction with an increase in the Reynolds number, while the transition of larger cylinder (D = 14mm) was observed in the early stage. It was found, therefore, that the variation of cylinder diameter has an effect on the transition phenomenon of the separated shear layer, and the heat transfer performance behind circular cylinders is influenced by its behavior.

INTRODUCTION

With a cylinder in crossflow, a boundary layer is formed on the front part as a result of the viscous forces and separates from its surface at a certain distance from the front stagnation point. Separated flows, which are caused in such a process, appear in heat exchangers and hot–wire anemometers. The design procedure of these instruments depends strongly on the understanding of heat transfer behavior and the specific feature of fluid dynamics. Accordingly, the problems of the separated flows are of interest in the fields of engineering and technology. The boundary–layer separation is roughly divided into two types: those of the laminar boundary layer and the turbulent boundary layer. Heat transfer and flow characteristics behind circular cylinders in both cases have been proposed by several authors. In particular, the heat transfer behavior due to the laminar boundary–layer separation is summarized by Zukauskas and Ziugzda(1).

In the situation that the laminar boundary layer is separated from the cylinder surface, it has been proposed in several articles (2,3,4) that heat transfer from circular cylinders is promoted by increasing free–stream turbulence. For the purpose of examining this result, the authors(5) also performed a similar experimental study. Their main attention was focused on the examinations of the heat transfer and flow characteristics on the rear part of a cylinder. As a result, it was found that if stream turbulence displays a high frequency, the heat transfer coefficient at the rear stagnation point is increased even at the lower turbulence level, which, according to the papers (2,3,4), has no effect on heat transfer. Further research(6), based on this result, was carried out. The data from that study showed that, even if a high frequency is not contained in free–stream turbulence in contrast with the above case, the heat transfer performance is influenced also by low frequency components and two patterns of heat transfer behavior are observed in the range of the Reynolds number from 7000 to 13000.

Meanwhile, Bloor(7) examined the character of the flow by using cylinders of different sizes under the constant Reynolds number condition. He concluded that, when the Reynolds number is over 1800, the change in cylinder size affects the length of the formation region of the vortices behind a circular cylinder. In such a variation, Gerrand(8) postulated that the scale length of the free–stream turbulence plays an improtant role in its region. On the other hand, the effect of cylinder size on heat transfer was not discussed in his paper. Judging from these results, it may be expected that the heat transfer performance on the rear part of a cylinder is changed corresponding to the variation of cylinder size.

From these points of view, this paper aims to clarify the flow and heat transfer characteristics caused by the laminar boundary–layer separation using circular cylinders of different diameters.

EXPERIMENTAL APPARATUS

Figure 1 shows the experimental apparatus used in the present study. Air is fed from a blast blower into a wind channel, which contains grids and screens to ensure a uniform velocity profile. The levels of turbulence and power spectrum were considerably adjusted with the relatively fine screens in the flow duct. The flow rate was controlled by a by–pass valve and the required Reynolds number was achieved by controlling its rate. After leaving the wind channel, the flow is introduced into a rectangular duct 1620mm in length with a square cross–section of 420mm×75mm. A test cylinder is set horizontally 300mm downstream from its entrance around which the air flows.

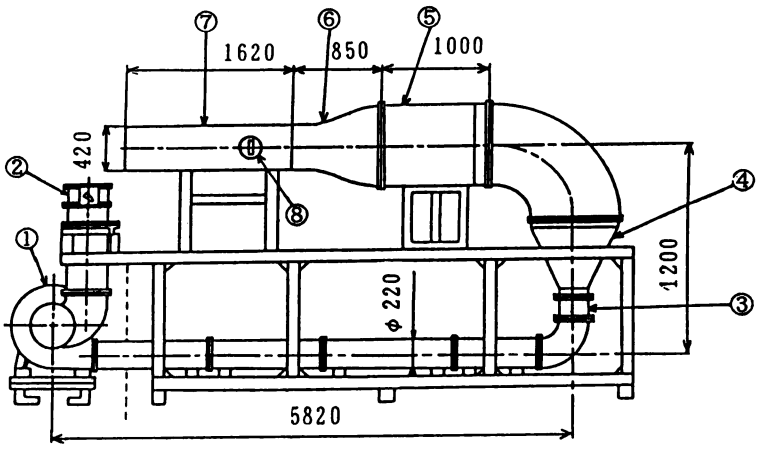

① Blower ② Butterfly-shaped valve
③ Multi-punched board ④ Diffuser
⑤ Settling chamber ⑥ Nozzle
⑦ Test section ⑧ Test cylinder

Fig. 1 Experimental apparatus

Two types of the test cylinders were used for the measurements of heat transfer and flow. One of these cylinders aims to examine the heat transfer characteristics around the cylinder. Thus the electrically heated cylinder shown in Fig.2 was formed in the following manner: the cylinder made of a bakelite bar is manufactured so as to form a spiral groove of 0.3mm pitch and 0.15mm in depth, and is

Table 1 Turbulence intensity

Re	Tu (%)		
	D = 10 mm	D = 12 mm	D = 14 mm
0.7×10^4	0.22	0.265	0.28
1.0×10^4	0.255	0.22	0.255
1.3×10^4 D = 10mm : 1.16×10^4	0.22	0.265	0.24

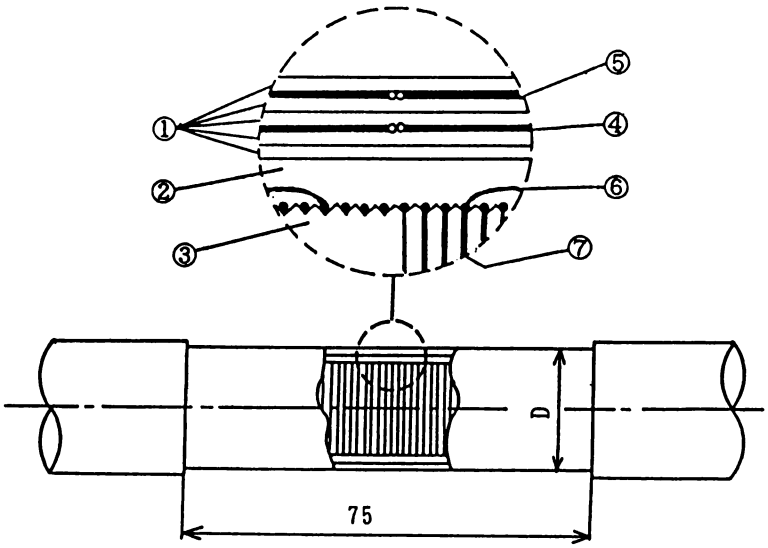

① Teflon tape ② Araldite ③ Bakelite bar
④ First thermocouple ⑤ Second thermocouple
⑥ Lead wire for measuring voltage
⑦ Chromel wire

Fig. 2 Detail of test cylinder

wound around its surface by use of a chromel wire 0.03mm in diameter. After that, the cylinder is covered with araldite 0.2mm thick. In order to estimate heat flux and wall temperature around the cylinder surface, two thermocouples of 0.03mm in diameter are used. As shown in Fig.2, one of thermocouples is fastened on the wall surface with a heatproof teflon tape 0.08mm thick, and the other is laid on top of its tape. Special care was taken in fixing the thermocouples on the same radius line. Heat flux and surface temperature were calculated from these two thermocbuple readings. The heated section formed in the above process is 75mm long. The chromel wire on the wall surface was heated using a DC generator, so a nearly constant heat flux condition was established along the cylinder. Nevertheless, the axial variation due to the heat conduction loss was detected on this surface. Accordingly,only the center portion, 10mm in length, was used as the test section for the heat transfer measurements. The other cylinder mentioned previously was prepared for the purpose of measuring pressure around

its wall surface, and is made of a brass tube with the same diameter as the heated cylinder. It is smoothly polished and has a 0.2–mm–diameter hole. To determine the circumferential pressure distribution, the test tube was rotated on its horizontal axis, and readings were taken at 5° intervals. A further measurement was introduced in order to examine the flow field behind the cylinder, which was made with the help of the hot–wire anemometer connected with an I–type probe. In this measurement, the power spectra of velocity fluctuation were obtained by analyzing the anemometer signal with a Fourier analyzer. Table 1 summarizes the level of turbulence in the test section. As is found from the table, turbulence of each cylinder is nearly maintained at the same level in the wide range of the Reynolds number. Corresponding power spectra of Re = 10000 are shown in Fig.3. In particular, the free–stream turbulence is adjusted in order to make its main component approach 10 Hz. Moreover, the peak value of turbulence is maintained at a constant level. The circular cylinders tested had a diameter of 10mm, 12mm and 14mm, respectively. The range of the Reynolds number (based on the cylinder diameter) was from 7000 to 13000.

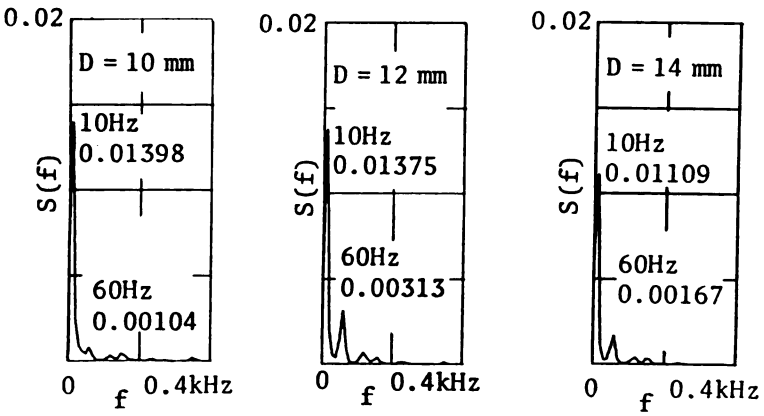

Fig. 3 Power spectrum of free–stream turbulence

By using cylinders of different diameters, the effect of a channel wall on heat transfer is expressed by the blockage factor, which is the ratio of the cylinder diameter to the channel height. Okamoto et al.(9) pointed out that, if the value of its factor is under 0.04, the effect of the duct wall is neglected. Predicating this condition, the blockage factor in the present study gives no influence on flow and heat transfer, because it is 0.0354 in the case of D = 14mm. Putting these situations together, it can be postulated that if no data are correlated in the same manner, the difference is effected by size.

EXPERIMENTAL RESULTS AND DISCUSSION

Nusselt number at the rear stagnation point and wall temperature distribution

Figure 4 summarizes the relation between the Nusselt number at the rear stagnation point and the Reynolds number for the three cylinders with different diameters. No data of Re = 13000 was obtained for the smaller diameter cylinder (D = 10mm) due to the limit in the capacity of the blower. Thus, corresponding data for Re = 11600 was used. The Nusselt number for each cylinder increased

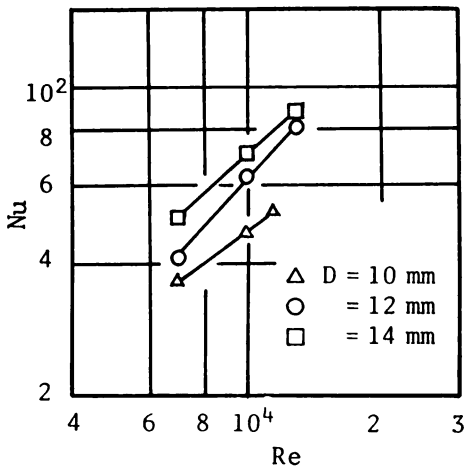

Fig. 4 Nusselt number at the rear stagnation point

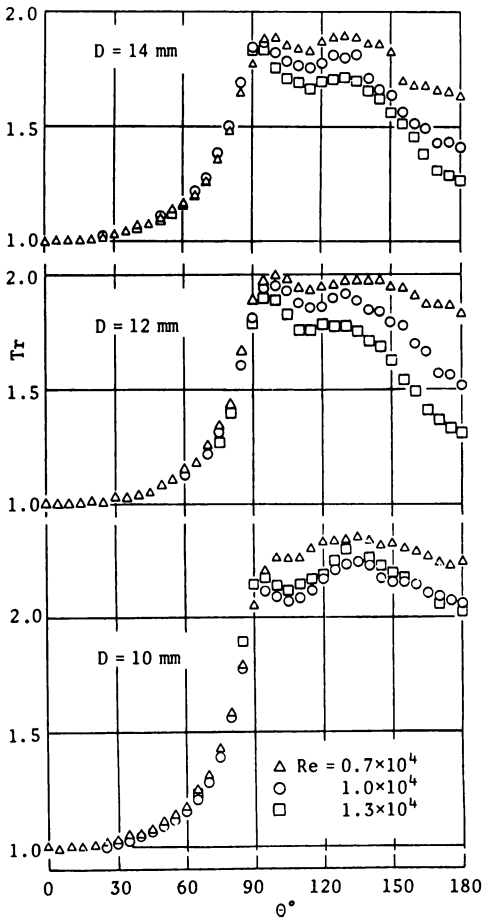

Fig. 5 Temperature distribution around a cylinder

as the Reynolds number increased and exhibited a line with a constant gradient. The result of the largest cylinder (D=14mm) shows a higher value than that of the other cylinders in the wide range of the Reynolds number, but the gradient parallels that of D=10mm. On the other hand, the behavior of D=12mm seems to be diffrernt from the above case, the Nusselt number of Re=7000 coincides nearly with the value of D=10mm, and that of Re=13000 seems to approach the data of D=14mm. Accordingly, the result of D=12mm is found to have a considerably larger gradient than that of the other cylinders.

Corresponding to the variation of the Nusselt number, temperature distribution around the cylinder is shown in Fig.5. The ordinate in the figure is the dimensionless value; the temperature difference between wall at a certain angle θ and free stream fluid is divided by that between wall at the front stagnation point and free stream fluid. The abscissa is the angle measured from the front stagnation point. On the front part of the cylinder, local wall temperatures are plotted as the same curve. The temperature distributions of all three cylinders have a maximum of $\theta=90^\circ$ after which a concave curve appears at $\theta=120^\circ$ at which point the surface temperatures decrease monotonously to the rear stagnation point. This variation for the smallest cylinder (D=10mm) is seen to be fairly gradual compared with that of D=12mm and D=14mm.

As seen in Figs.4 and 5, the heat transfer behaviors behind the cylinders seem to be influenced by the variation of the cylinder size. Based on this situation, it is found that the cylinder size also influences the structure of the fluid dynamics. According to the experimental result obtained by Fuse et al. (5), heat transfer in the rear part of the cylinder is highly dependent on characteristics of the separated shear layer. Moreove, pressure distribution on the cylinder surface constitutes one of the important structural parameters of the flow. Considering these variables, the effect of the cylinder size on heat transfer will be examined in the following section through measurements of the pressure around the cylinder and the separated shear layer.

Pressure distribution

Figure 6 shows the circumferential distribution of the pressure on the test cylinder. The ordinate is the pressure coefficient; the difference between the measured value and the static pressure in the free stream is divided by the dynamic pressure. As shown in Fig.6, the pressure decreases sharply in the front zone of the cylinder and falls to a minimum. After that, it begins to increase with the angular distance and gradually approaches a constant level. It can be approximately estimated from the figure that, although no measurement was performed regarding the friction stress on the cylinder surface, the separation point is located in the pressure recovery region. Therefore this streamwise variation is surely caused by the laminar boundary–layer separation. Such a distribution is observed in all three cylinders in the wide range of the Reynolds number. In particular, the figure shows that the pressure variation on the front part is produced in the same manner. This fact suggests that heat transfer in the front region would not be affected by either the cylinder size or the Reynolds number. For the relatively low Reynolds number (Re=7000), the pressures for D=10mm and D=12mm show the same value at each location around the cylinder, while the result of D=14mm is lower than that of the other cylinders in the range of 60° to the rear stagnation point. In the higher Reynolds number, the result of D=12mm forms a prominent contrast to the above case, and expresses the same distribution as that of the largest cylinder. From these results, it could be postulated that the distribution of D=12mm is gradually shifted to that of D=14mm with an increase in the Reynolds number, which corresponds to the variation of the Nusselt number mentioned previously.

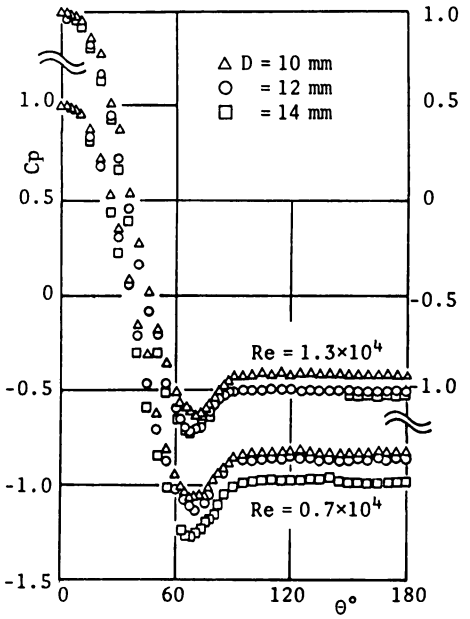

Fig. 6 Pressure distribution around a cylinder

Characteristics in the separated shear layer

Prior to the examination for characteristics of the separated shear layer formed behind the cylinder, the formation of this layer was estimated from transverse profile of the streamwise velocity. For this measurement, the sensor of the hot-wire anemometer at each axial location was moved across the rectangular channel using a traversing device. As an example, measured profiles of D = 14mm are summarized in Fig.7 for the case of Re = 10000. No data in the vicinity of the rear stagnation point can be regarded as the streamwise velocity, since a reverse stream appears in this region. Adachi et al.(10) defined the thickness of the separated shear layer at a certain location according to the velocity profile. Thickness corresponds to a distance between transverse locations of a minimum and a maximum of the streamwise velocity. Since this idea has been widely accepted, the poor measurement accuracy mentioned above may have no direct influence on the estimation of the separated layer thickness. In the present study, therefore, the formation of the separated shear layer has been evaluated based on the above manner.

Obtained profile for each cylinder is shown in Fig.8 in the form of vertical distance Y/D vs. downstream distance X/D, where the results of the different Reynolds numbers are included. Dash–dotted, solid and dotted lines represent data of D=10mm, D=12mm and D=14mm, respectively. For the relatively low Reynolds number (Re=7000), the profiles of D=10mm and D=12mm illustrate the same variation along the flow. On the other hand, a prominent difference is found for the case of the largest cylinder: the thickness of the separated layer increases considerably in the streamwise direction compared with the other cases. Corresponding results of Re = 10000 show a smooth and gradual increase in the shear thickness along the axis X/D with the cylinder size. As

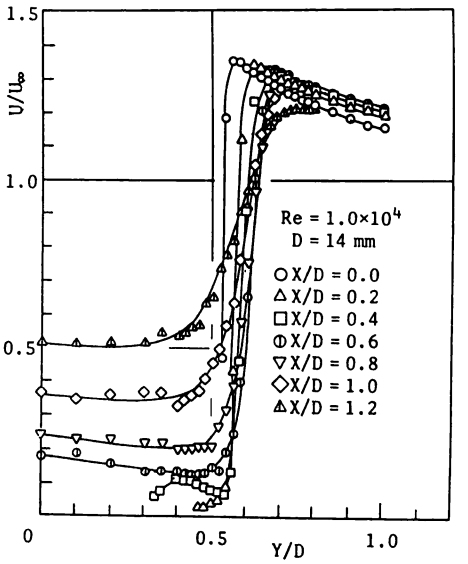

Fig. 7 Streamwise velocity profiles (Re=10000 for D=14mm)

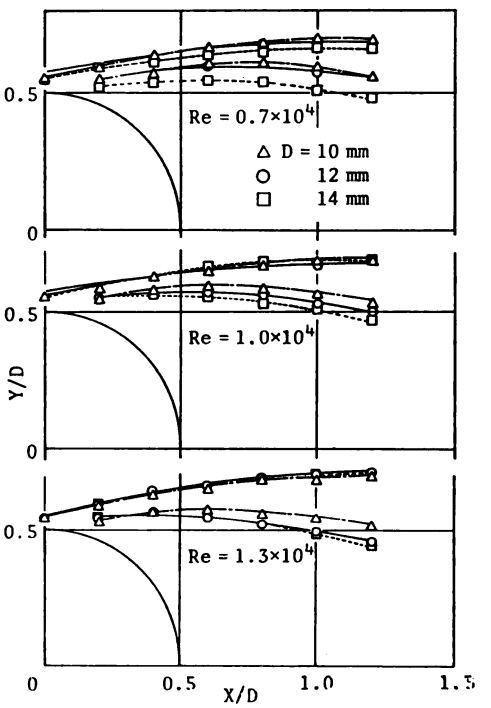

Fig. 8 Formation of the separated shear layer

shown in the lowest part of Fig.8, the results of the higher Reynolds number have a contrast to the case of Re=7000, and the streamwise profile of D=12mm is similar to that of D=14mm rather than D=10mm. The profiles indicate that the separated layer thickness of each cylindder increases with the Reynolds number in the flow direction. The degree of its streamwise spread seems to become larger in the case of D=12mm. Throughout these results, the formations of the separated shear layer behind the cylinders were determined and examined to a certain extent. Thus an attempt was turned to clarify the characteristics in each layer.

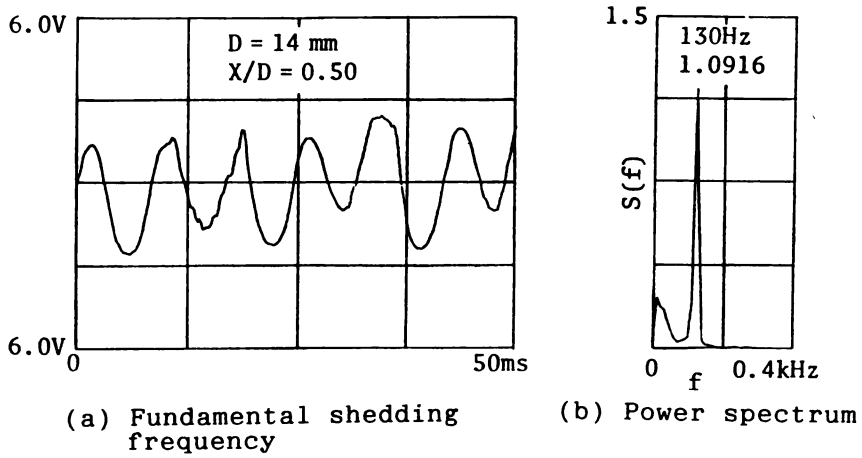

Fig. 9 Longitudinal velocity fluctuation in the separated shear layer
(a) Fundamental shedding frequency
(b) Power spectrum

Fig.9 (a) and (b) show longitudinal velocity fluctuation in the separated shear layer and its power spectrum, which were measured at a location 0.5D downstream from the center of the cylinder. The ordinate in (b) of Fig.9 is the power spectrum and its scale is random. Sinusoidal oscillations in (a) of Fig.9 present vortex shedding waves. Frequency estimated from these waves corresponds to the maximum value of the power spectrum shown in (b) of the figure, and is the so–called fundamental shedding frequency.

Following the above measurement, the streamwise variation of a maximum value of the power spectrum at each streamwise location is summarized in Fig.10 for three cylinder. The formation region of vortices behind the cylinder has been studied so far by several authors. Moreover, it is well known that, if the laminar boundary–layer separation occurs in the front part of the cylinder, the transition from laminar to turbulent flow always appears in the separated shear layer. However, no widely accepted definition for this transition seems to be specified.

Bloor (7) proposed that, when the transition phenomenon occurs, a relatively high frequency is observed in waves of the vortex shedding, which is called transition waves. Furthermore, he mentioned that the onset of the laminar–to–turbulent transition is determined by the first appearance of these waves, and when the fundamental frequency is almost masked, the flow degenerates perfectly to turbulence. At this stage, however, it would be impossible to discuss validity of this definition. Accordingly the above idea was used in the present study. Obtained locations for the beginning of the transition phenomenon and its end are plotted in the Fig.10 with half open and solid circles. The streamwise region between two symbols corresponds to the transition region.

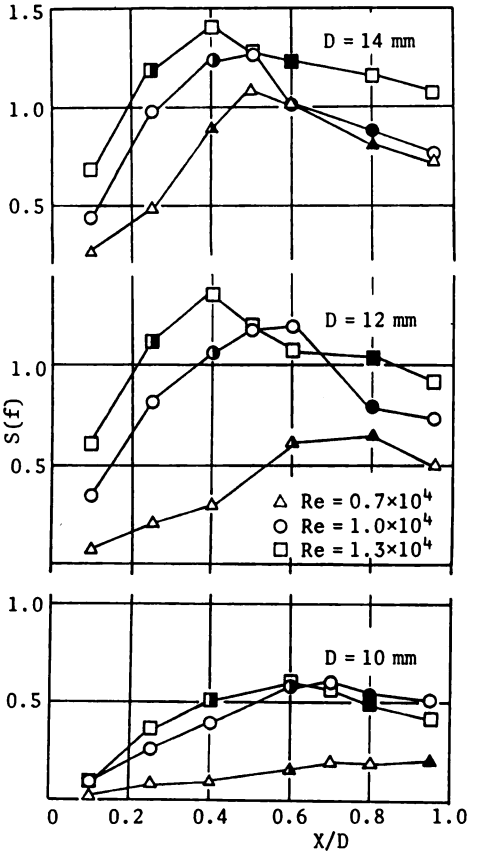

Fig. 10 Streamwise Variation of power spectrum

As show in Fig.10, the maximum value of the power spectrum at each location increases in the first stage. Subsequently it begins to decrease gradually along the flow except the data of Re=7000 in the lowest part of the figure. A peak of data, which appears in the streamwise direction, is seen to locate in the transition region. This location is shifted upstream due to an increase in the Reynolds number and/or the cylinder size. In other words, the transition to turbulence occurs in the initial stage according to the increase in these two factors.

Generally speaking, if the laminar–to–turbulent transition occurs in the relatively earlier stage, an exchange of momentum between the vortex wake and the free stream is made in an active manner, so that the vorticity begins to diffuse from the vicinity of the separation point. It may be postulated, based on this idea, that the variation of vorticity corresponds to the above result that the dramatic change for the transition to turbulence takes place near the cylinder as the Reynolds number is increased from 7000 to 13000 and/or the cylinder diameter is changed from 10mm to 14mm. Correspondingly, if momentum is exchanged at the higher level between outer and inner regions of the separated layer, heat transfer behind the cylinder may be promoted due to this effect. As mentioned previously, the transition region of D=10mm locates downstream compared to the case of D=14mm. The corres-

ponding Nusselt number for the smallest cylinder is rather lower than other cylinder cases. It can be concluded, therefore, that the heat transfer characteristics on the rear part of the cylinder are dominated by a shift of the transition region, and the earlier transition leads to an increase in the separated layer thickness.

Putting the above discussions trgether, a further examination was made on the behavior of the Nusselt number(D=12mm). The streamwise power spectrum distribution in this case is similar to that of D=10mm in the lower Reynolds number region, and comes to resemble the profile of D=14mm as the Reynolds number increases. It is found from Fig.10, therefore, that, if a discussion is made in the same Reynolds number region, the result of D=12mm shows a clearer trend than these of the other cylinders. Throughout the results of Fig.6 and Fig.9, this behavior for the power spectrum corresponds also to the results of the pressure distributions and the profiles of the separated shear layer. From the viewpoint of these results, it is apparent that the substantial change in heat transfer of D=12mm is related to the rapidly upstream shift of the transition region compared with the other cylinder cases.

SUMMARY

An experimental study was performed on heat transfer and flow characteristics behind cylinders with three different sizes. Obtained results are summarized as follows.

(1) The Nusselt numbers at the rear stagnation point increase linearly with the Reynolds number and/or the cylinder size. Correspondingly, the distributions of temperature and pressure around the cylinder also are influenced due to these factors.

(2) The laminar–to–turbulent transition appears in the separated shear layer and its region is shifted upstream with the increase in the Reynolds number and cylinder size. Therefore, the heat transfer and flow characteristics on the rear part of the cylinder are related to the transition phenomenon in the separated shear layer.

NOMENCLATURE

Cp	pressure coefficient $=(P-P_f)/(\rho U^2/2)$
D	diameter of circular cylinder, mm
f	frequency
h	local heat transfer coefficient around cylinder, $W/(Km^2)$
L	length between both walls of rectangular duct, mm
Nu	Nusselt number $=hD/\lambda$
P	local pressure on cylinder surface, Pa
Pf	static pressure of free stream, Pa
Re	Reynolds number $=UD/\gamma$
S(f)	power spectrum
T	local wall temperature of cylinder, K
T_f	fluid temperature of free stream, K
T_r	temperature ratio $=(T-T_f)/(T_s-T_f)$
T_s	surface temperature at the front stagnation point, K
Tu	turbulence intensity $=(u^2)^{0.5}/U$
t	time, s
U	free–stream velocity, m/s

$\bar{U}$ time–averaged velocity in the streamwise direction, m/s

u longitudinal component of the velocity fluctuation, m/s

X Cartesian coordinate in the mean flow direction

Y Cartesian coordinate normal to free stream

Greek letters

ρ density, kg/m^3

γ kinematic viscosity, m^2/s

λ thermal conductivity, W/m/K

θ angle measured from the front stagnation point of circular cylinder

REFERENCES

1) Zukauskas, A. and Ziugzda, J., Heat transfer of a cylinder in crossflow, Springer–Verlag, Berlin, 1985.

2) Comings, E. W., Clapp, J. T. and Taylor, J. F., "Air turbulence and transfer process (Flow normal to cylinders)," Ind. Engng Chem, Vol.40, 1948, pp.1076–1088.

3) Pertrie, A. M. and Simpson, H. C., "An experimental study of the sensitivity to free–stream turbulence of heat transfer in wakes of cylinders in crossflow," Int. J. Heat Mass Transfer, Vol.15, No.8, 1972, pp.1497–1513.

4) Boulos, M. I. and Pei, D. C. T., "Dynamics of heat transfer from cylinders in a turbulent air stream," Int. J. Heat Mass Transfer, Vol.17, No.7, 1974, pp.767–783.

5) Fuse, H., Oyama, T. and Kanamori, S., "Influence of Free–Stream Turbulence on Heat Transfer at the Rear Surface of a Cylinder," Trans. Jpn. Soc. Mech. Eng., (in Japanese), Vol.50, No.453, B, 1984, pp.1302–1309.

6) Fuse, H., Oyama, T., Niihara, O. and Uchiyama, Y., "Free–stream Turbulence on Heat Transfer in the Separated Region of a Circular Cylinder," Trans. Jpn. Soc. Mech. Eng., (in Japanese), Vol.51, No.470, B, 1985, pp.3392–3396.

7) Bloor, M. S., "The Transition to Turbulence in the Wake of a Circular Cylinder," J. Fluid Mech, Vol.19, No.2, 1964, pp.290–304.

8) Gerrand, J. H., "The Mechanics of the Formation Region of Vortices behind Bluff Bodies," J. Fluid Mech, Vol.25, No.2, 1966, pp.401–413.

9) Okamoto, T. and Takeuchi, Y., "Effect of Duct Wall on flow around a cylinder and its wake," Trans. Jpn. Soc. Mech. Eng., (in Japanese), Vol.41, No.341, 1975, pp.181–188.

10) Adachi, T. and Kato, E., "Study on the Flow about a Circular Cylinder in Shear Flow," J. Jpn. Soc. Aer. Spa. Soc., (in Japanese), Vol.23, No.256, 1975, pp.45–53.